Spreading Dynamics of a Viral Infection in a Complex Network

Khemanand Moheeput, Smita S. D. Goorah, and Satish K. Ramchurn

Abstract—We report a computational study of the spreading dynamics of a viral infection in a complex (scale-free) network. The final epidemic size distribution (FESD) was found to be unimodal or bimodal depending on the value of the basic reproductive number R_0. The FESDs occurred on time-scales long enough for intermediate-time epidemic size distributions (IESDs) to be important for control measures. The usefulness of R_0 for deciding on the timeliness and intensity of control measures was found to be limited by the multimodal nature of the IESDs and by its inability to inform on the speed at which the infection spreads through the population. A reduction of the transmission probability at the hubs of the scale-free network decreased the occurrence of the larger-sized epidemic events of the multimodal distributions. For effective epidemic control, an early reduction in transmission at the index cell and its neighbors was essential.

Keywords—Basic reproductive number, epidemic control, scale-free network, viral infection.

I. INTRODUCTION

COMPLEX networks contemporarily underpin significant research in the description of infectious diseases and their control [1]. We report a computational study of the spreading dynamics of a viral infection in a complex (scale-free) network [2] defined on a real-life human population distribution. The dynamics was simulated using a stochastic discrete-time susceptible-exposed-infected-removed (SEIR) cellular model. The basic reproduction number, R_0, was computed as the average number of secondary cases (average taken over all the stochastic realizations) produced by an index case during its infectious period in an otherwise totally susceptible population. The final epidemic size distribution (FESD) was found to be unimodal or bimodal depending on the value of R_0. R_0 increased linearly with the transmission probability with a gradient equal to the product of the infectious period and the average daily number of contacts of the index case during this length of time. The FESDs occurred on time-scales long enough for intermediate-time epidemic size distributions (IESDs) to be important in the implementation of control

Khemanand Mooheput is with the Department of Physics, Faculty of Science, University of Mauritius, Reduit, Mauritius (e-mail: moheeputk@gmail.com).
Smita S. D. Goorah is with the Department of Medicine, Faculty of Science, University of Mauritius, Reduit, Mauritius (e-mail: sm.goorah@uom.ac.mu).
Satish K. Ramchurn is with the Department of Physics, Faculty of Science, University of Mauritius, Reduit, Mauritius (e-mail: satish.ramchurn@gmail.com).

measures. The usefulness of R_0 for deciding on the timeliness and intensity of control measures was found to be limited by the multimodal nature of the IESDs and by its inability to inform on the speed at which the infection spreads through the population noting that, for a fixed value of R_0, different stochastic realizations spread at different speeds. It was also found that a reduction of the viral transmission probability at the hubs of the scale-free network decreased the occurrence of the larger-sized epidemic events of the multimodal distributions but that for effective epidemic control an early reduction in transmission at the index cell and its neighbors is essential thus highlighting the need for a strong public health surveillance system for an early identification of the index case and rapid intervention for efficient epidemic mitigation and control.

II. METHODS AND DESCRIPTION OF MODEL

A. Geographical Region of Interest

The viral propagation was assumed to have started following the introduction of an index infected human case into a totally susceptible human population located in an area of interest of Port Louis, the capital city of Mauritius. The area of interest was selected from a Google Earth digital image of the city. This area was the same as that previously used to study an outbreak of dengue fever in Mauritius [3]. The area of interest, of size $(2.9\,km \times 3.6\,km)$, was divided into cells each of size $(0.1\,km \times 0.1\,km)$. The number of houses in each cell was estimated using color image analysis. The human population distribution was then obtained by assuming an average number of five inhabitants per house.

B. The Scale-Free Network

The scale free network was set up as as follows [3]:
1. Four most frequently visited places (primary hubs) in the area of interest were chosen.
2. Each hub was represented by one cell.
3. The index cell was randomly linked to two of the hubs.
4. Another cell was chosen. The cell was allowed to link itself with the hubs or with the index cell using the Barabási–Albert algorithm [2].
5. The procedures 3-4 were repeated for the remaining cells to generate a scale-free network [2].

C. Human Interaction and Infection Model

The index case was assumed to reside in an index cell. Individuals in a cell were assumed to interact with each other

using an SEIR (susceptible-exposed-infected-removed) human interaction model. The probability, p_{IS}, that a susceptible individual was infected by contact with n_i infectious individuals was $p_{IS} = 1 - (1 - \lambda)^{n_i}$, where λ is the transmission probability on contact. This infection was accepted provided p_{IS} was greater than a uniform $(0, 1)$ random number and the susceptible individual then moved to the exposed (latent) state before moving to the infectious state and then to the recovered state. The latent period was 5 days and the infectious period was also 5 days. The incubation period was assumed to be 6 days. The latent period was chosen to be equal to the infectious period so that the index case was the only infectious human in the population during the infectious period of this individual. This allowed a straightforward computation of the basic reproductive number. The number of contacts of the index case during its infectious period was the number of random numbers generated during this length of time.

D. Human Mobility Model

Individuals in a cell were also assumed to be able to move locally with equal probability to each of the eight next neighboring cells and interact with individuals of those cells. They were also assumed to move globally on the scale-free network and interact with individuals on the network. Only 10% of the human population of a cell was allowed to move globally (and 10% locally) at each time step (one day) and they returned to their original cell at the end of the time step.

E. Stochastic Realization

A run of an SEIR simulation was assumed completed after the update of the status of all the individuals in the area of interest. Each run corresponded to a time-step of one day. A stochastic realization of the simulation covered a length of time sufficient for the epidemic to converge to its final epidemic size for that simulation. This length of time depended on the value of the transmission probability. An epidemic size distribution was taken as the distribution of the epidemic size over all the stochastic realizations at an arbitrary time. The final epidemic size distribution was the converged epidemic size distribution.

F. Calculation of the Basic Reproduction Number

Let r be the number of secondary cases produced by the index case during its infectious period in an otherwise totally susceptible population in a stochastic realization and r_i be the value of r in the ith stochastic realization. Then, the basic reproduction number (R_0) was taken as the average of r over all the stochastic realizations. Thus, for N stochastic realizations,

$$R_0 = <r> = \frac{1}{N}\sum_{i=1}^{N} r_i$$

G. Epidemic Control Strategy

The epidemic control strategy involved (i) a reduction of the transmission probability at the hubs of the network right from the introduction of the index case in the human population and/or (ii) a reduction of the transmission probability at source, i.e. at the index cell and its surrounding cells, as from the end of the incubation period.

III. RESULTS

The human population size for the area of interest was computed as 82,580 and this was heterogeneously distributed over the area. For example, the index cell was found to have a population of 165 humans while the populations of the 4 primary hubs were 255, 215, 195 and 35. The primary hubs had 82, 44, 35 and 18 links from the most connected to the least connected hub. It was also found that a number of hidden hubs [4] arose from the construction of the network. These hubs are cells, other than the primary hubs, which by virtue of the construction of the scale-free network developed a large number of links compared to other cells. Table I shows the cell-link distribution for the network, for cells other than the primary hubs.

TABLE I
CELL-LINK DISTRIBUTION FOR THE SCALE-FREE NETWORK CONSTRUCTED, FOR CELLS OTHER THAN THE PRIMARY HUB

No. of links	1-5	6-10	11-15	16-20	21-25	26-30	31-35	36-40
No. of cells	604	29	13	3	2	1	1	1

The final epidemic size, i.e. the average of the final epidemic size distribution, increased with the transmission probability. Fig. 1 shows the final epidemic size distributions for transmission probabilities of $\lambda = 10^{-3}, 2 \times 10^{-3}, 5 \times 10^{-3}$ and 1×10^{-2} for 500 stochastic realizations.
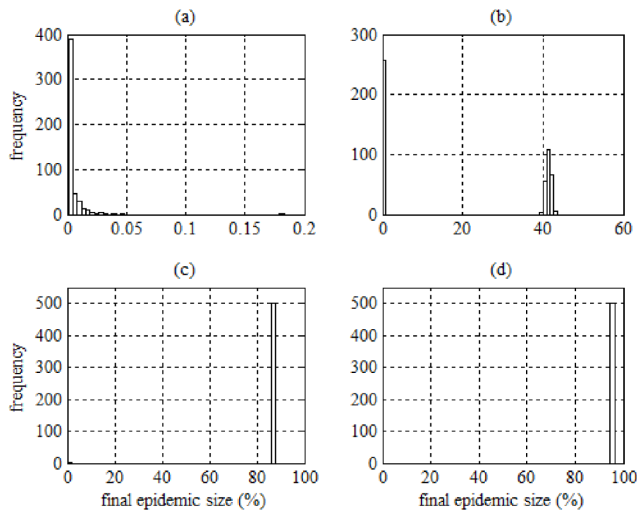
Fig. 1 Histograms of the final epidemic size (expressed as % of the total population) distributions for (a) $R_0 = 0.8680$, (b) $R_0 = 1.7260$, (c) $R_0 = 4.6571$ and (d) $R_0 = 8.7240$. The number of stochastic realizations was 500 for each value of R_0
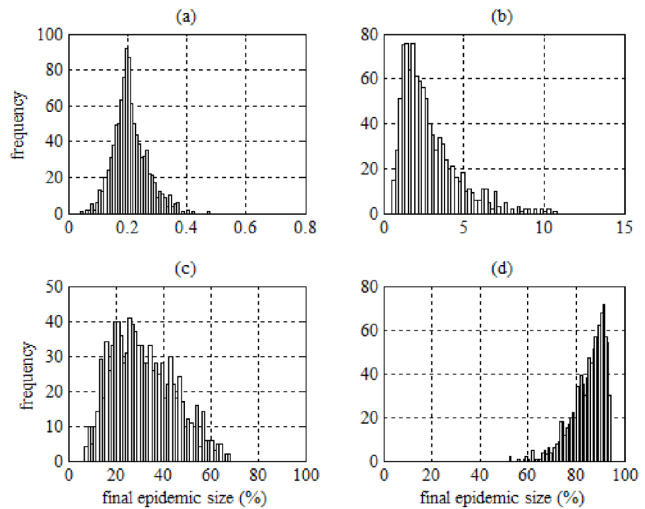

Fig. 2 Epidemic evolution for $R_0 = 8.7240$: temporal histograms of epidemic sizes for 1000 stochastic realizations at (a) 20 days, (b) 40 days, (c) 60 days and (d) 80 days

The times taken for convergence of the distributions depended on λ and were respectively 200, 650, 200 and 150 days for these values of λ. The associated values of the basic reproductive number were $R_0 = 0.8680, 1.7260, 4.6571$ and 8.7240. For these values of R_0, the epidemic size distributions were sizeable for only $R_0 = 1.7260$ (bimodal) and $R_0 = 4.6571$ (unimodal) and $R_0 = 8.7240$ (unimodal). Although the final epidemic size distributions were either bimodal or unimodal, the distributions displayed multimodal behaviour as the epidemic developed as shown in Fig. 2 for $R_0 = 8.7240$ for 1000 stochastic realizations.

At 60 days, for example, the epidemic size was a multi-valued function of r as shown in Fig. 3 for $R_0 = 8.7240$.
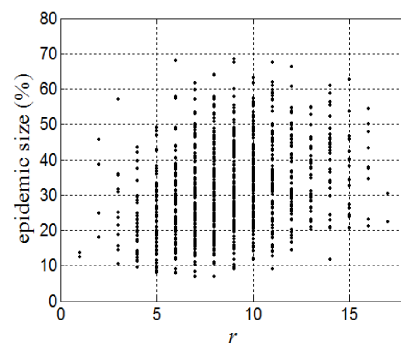

Fig. 3 Epidemic size as a function of r (as defined in the text) for 1000 stochastic realizations at 60 days for $R_0 = 8.7240$

Thus, at 60 days, for $R_0 = 8.7240$ and a fixed value of r, different stochastic realizations can yield different epidemic sizes whereas the same epidemic sizes can be obtained from different values of r. The above results also show that R_0 increased linearly with the transmission probability with a gradient equal to 877. The average daily number of contacts of the index case during its infectious period was found to be 175.

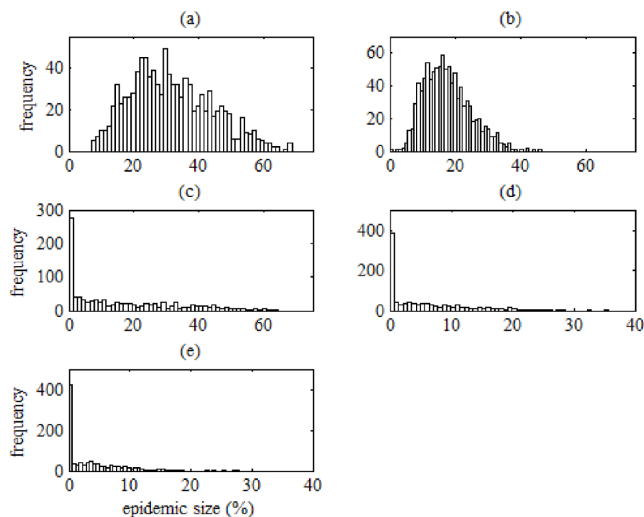The results of various epidemic control strategies are shown in Fig. 4 for $R_0 = 8.7240$.

Fig. 4 Histograms showing effects of various control strategies on the epidemic size at 60 days for $R_0 = 8.7240$: (a) no intervention, (b) interventions at the primary hubs from the start of the simulations, (c) interventions at the index cell and its 8 immediate neighbors as from the 7th day of the simulations, (d) the combination of (b) and (c), (e) the combination of (b) and (c) together with interventions at the hidden hubs from the start of the simulations. The number of stochastic realizations was 1000 in each case

The locations of the primitive hubs were known by construction and thus interventions consisting of the reduction of the transmission probability by a factor of 100 were applied from the first day of the simulations. As Fig. 4 (b) shows, these interventions led to a reduction of the frequency of the larger-sized epidemic events. However, interventions at the index cell and its 8 immediate neighbors as from the 7th day, i.e. as from the end of the incubation period, had a much more significant impact on the epidemic size distributions as shown in Fig. 4 (c). This impact is enhanced by a combination of interventions at the index cell, its 8 immediate neighbors and the primitive hubs (Fig. 4 (d)) and further enhanced by a combination which also includes interventions at the hidden hubs (Fig. 4 (e)) where we took the hidden hubs as those cells, other than the primary hubs, which has greater of equal to 16 links.

IV. DISCUSSION

Public health planning and response to the threat of emerging and re-emerging viral infections depend to a large extent on our ability to forecast and minimize the size of epidemics. With the advent of modern computational facilities, sophisticated computing techniques and network epidemiology [5], useful models for the mapping and forecasting of epidemics in realistic human populations are being developed and used for simulations. The model used here combines stochastic cellular automata and scale-free network epidemiology with Google Earth satellite imagery to map the development of an infection in a real-life human population and forms part of a suite of some recent models [3], [6-8]

using open-source satellite imagery for infectious disease mapping and control.

The model generates unimodal or bimodal final epidemic size distributions, depending on the value of R_0. However, the time taken to reach the final epidemic size occurs on time-scales long enough for epidemic size distributions at intermediate times to be important in the implementation of control strategies. The intermediate-time epidemic size distributions were found to be multimodal with large variances. Such distributions limit the usefulness of R_0 as a decision-making tool for judging on the timeliness and intensity of control measures. This limitation is compounded by the fact that, for the same value of R_0, different stochastic realizations spread at different speeds and that only one of the stochastic realizations will occur. Moreover, the linear dependence of R_0 on λ descends from the infection model which ensures that when $n_i = 1$, $p_{IS} = \lambda$ and the infection would be accepted for λ times the number of contacts with the result that R_0 would then be equal to the product of λ, the infectious period and the average daily number of contacts.

The idea of controlling the spread of epidemics in scale-free networks by hub-targeting is widely discussed in the literature [4], [9]-[12] In this study, a 100-fold reduction of viral transmission probability at the hubs decreased the occurrence of the larger-sized epidemic events but for a really effective epidemic control an early reduction in transmission at the index cell and its neighbours is essential. Tardy identification and implementation of control measures can only lead to larger epidemic sizes and weaker public health responses with increased morbidity and social distress. This highlights the need for the strengthening of public health systems for early identification of index cases and rapid interventions for efficient epidemic mitigation and control.

REFERENCES

[1] V. Colizza, M. Barthélemy, A. Barrat and A. Vespignani, "Epidemic modeling in complex realities," C. R. Biologies vol. 330, pp 364–374, 2007.
[2] A-L. Barabási, R. Albert and H. Jeong, "Mean-field theory for scale-free random networks," Physica A vol. 272, pp 173-87, 1999.
[3] S. K. Ramchurn,, K. Moheeput and S. S. Goorah, "An analysis of a short-lived outbreak of dengue fever in Mauritius," Euro. Surveill. vol. 14, pii = 19314, 2009.
[4] Y. Wanga, G. Xiao, J. Hua, T. H. Chenga and L. Wang, "Imperfect targeted immunization in scale-free networks," Physica A vol. 388, pp. 2535-2546, 2009.
[5] L. Danon, A. P. Ford, T. House, C. P. Jewell, M. J. Keeling, G. O. Roberts, J. V. Ross and M. C. Vernon, "Networks and the epidemiology of infectious disease," Interdiscip. Perspect. Infect. Dis. 284909 2011.
[6] A. Chang, M. Parrales, J. Jimenez, M. Sobieszczyk, S. Hammer, D. J. Copenhaver and R. P. Kulkarni, "Combining Google Earth and GIS mapping technologies in a dengue surveillance system for developing countries," Int. J. Health Geogr. vol. 8, 49 2009.

[7] R. Kamadjeu, "Tracking the polio virus down the Congo River: A case study on the use of Google Earth in public health planning and mapping," Int. J. Health Geogr. vol 8, 4 2009.

[8] S. Lozano-Fuentes, D. Elizondo-Quiroga, J. Farfan-Ale, M. Lorono-Pino, J. Garcia- Rejon, S. Gomez-Carro, et al., "Use of Google Earth to strengthen public health capacity and facilitate management of vector-borne diseases in resource-poor environments.," Bull. WHO vol. 86, pp. 718–725, 2008.

[9] Z. Dezső, and A-L Barabási, "Halting viruses in scale-free networks," Phys. Rev. E vol. 65, 055103(R) 2002.

[10] R. Pastor-Satorras and A. Vespignani, "Immunization of complex networks," Phys. Rev. E vol. 65, 036104 2002.

[11] F. Nian and X. Wang, "Efficient immunization strategies on complex networks," J. Theor. Biol. vol. 264, pp. 77–83 2010.

[12] H. Zhang, J. Zhang, C. Zhou, M. Small and B. Wang, "Hub nodes inhibit the outbreak of epidemic under voluntary vaccination.," New J. Phys. vol. 12, 023015 2010.